Localized and nonspreading spatiotemporal Wannier wave packets in photonic crystals

Stefano Longhi
Dipartimento di Fisica and Istituto di Fotonica e Nanotecnologie del CNR, Politecnico di Milano, Piazza L. da Vinci 32, I-20133 Milan, Italy

(Received 2 August 2004; revised manuscript received 23 September 2004; published 10 January 2005)

A general analysis of undistorted propagation of localized wave packets in photonic crystals based on a Wannier-function expansion technique is presented. Different kinds of propagating and stationary spatiotemporal localized waves are found from an asymptotic analysis of the Wannier function envelope equation.

DOI: 10.1103/PhysRevE.71.016603 PACS number(s): 41.20.Jb, 42.70.Qs, 42.25.Bs

I. INTRODUCTION

Spatiotemporal broadening of localized wave packets with finite energy due to the effects of diffraction and dispersion is a universal and challenging phenomenon in any physical context involving wave propagation. If the finite energy constraint is left, special spatiotemporal waves with a certain degree of localization in space and/or in time, capable of propagating free of diffraction and/or temporal dispersion, can be constructed. Localized waves of this type include, among others, Bessel beams, focus-wave modes, X-type waves, and pulsed Bessel beams [1–5]. Though these waves can be only approximately realized in practice, several experiments in acoustic and optical fields have been reported so far showing nearly-undistorted localized wave propagation. As the existence of undistorted progressive localized waves in vacuum has been known for many years and lead to long-standing studies [1,2], with special attention devoted toward their superluminal or subluminal character and to their finite-energy realizations, in the past few years these studies have been extended to dispersive optical media [3–5], and remarkably the spontaneous generation of localized and nonspreading wave packets mediated by optical nonlinearities has been predicted [6] and experimentally observed [7] using standard femtosecond pulsed lasers. Very recently, in a few works [8–10] the issue of spatial or spatiotemporal wave localization in *periodic* media has been addressed, and the possibility of exploiting well-established anomalous diffractive and dispersive properties of photonic crystals (PCs) [11,12] to induce novel spatiotemporal wave localization mechanisms has been proposed. Specifically, these studies have been concerned with localization of Bose-Einstein condensates in a one-dimensional optical lattice without any trapping potential [8], with two-dimensional (2D) spatial Bessel X waves in weakly coupled 2D waveguide arrays showing bidispersive properties [9] and with three-dimensional (3D) out-of-plane X-wave localization in 2D PCs [10]. Spatiotemporal waves considered in these works rely on some specific models and often use *ad hoc* approximations, e.g., reduced coupled-mode equations, paraxiality, weak-coupling limit, and continuum approximations. So far, a general framework to capture spatiotemporal wave localization and propagation in PCs and the derivation of a general wave equation, valid regardless of the specific system under investigation and with a wide range of applicability, is still lacking.

The aim of this work is to provide a general analytical framework to study spatiotemporal wave propagation in 2D and 3D PCs based on the use of Wannier functions, which have been introduced in the context of PCs to treat localized modes, such as the bound states of impurities or lattice defects [13–15]. A general asymptotic analysis of the envelope equation for the Wannier functions allows one to capture the existence and properties of localized nonspreading wave packets in PCs in terms of localized solutions of canonical wave equations, such as the Schrödinger equation, the Helmholtz equation and the Klein-Gordon equation.

II. WANNIER FUNCTION ENVELOPE EQUATION

The starting point of the analysis is provided by the vectorial wave equation for the magnetic field $\mathbf{H}=\mathbf{H}(\mathbf{r},t)$ in a PC with a periodic relative dielectric constant $\epsilon(\mathbf{r})$,

$$\nabla \times \left(\frac{1}{\epsilon} \nabla \times \mathbf{H} \right) = -\frac{1}{c^2} \frac{\partial^2 \mathbf{H}}{\partial t^2}, \tag{1}$$

where c is the speed of light in vacuum. In writing Eq. (1), we assumed that the material dispersion can be neglected, which is a reasonable assumption since in PCs with a relatively strong contrast index band dispersion broadly dominates over intrinsic material dispersion. To study the propagation of a spatiotemporal wave packet, we can adopt the method of the Wannier functions, which is commonplace in the study of the quasi-classical electron dynamics in solids [16,17] and recently applied to study localized modes and defect structures in PCs with defects [13,14]. We refer explicitly to a 3D PC structure, however a similar analysis can be developed for a 2D PC. Let us first consider the monochromatic Bloch-type solutions to Eq. (1) at frequency ω, $\mathbf{H}(\mathbf{r},t)=\mathbf{H}_{\mathbf{k},n}(\mathbf{r})\exp(-i\omega t)$, where $\mathbf{k}$ lies in the first Brillouin zone of the reciprocal $\mathbf{k}$ space, $\omega=\omega_n(\mathbf{k})$ is the dispersion curve for the nth band, and $\mathbf{H}_{\mathbf{k},n}(\mathbf{r})$ are the band modes, satisfying the condition $\mathbf{H}_{\mathbf{k},n}(\mathbf{r}+\mathbf{R})=\mathbf{H}_{\mathbf{k},n}(\mathbf{r})\exp(i\mathbf{k}\cdot\mathbf{R})$ for any lattice vector $\mathbf{R}$ of the periodic dielectric function. The Bloch functions $\mathbf{H}_{\mathbf{k},n}(\mathbf{r})$ are normalized such that $\langle \mathbf{H}_{\mathbf{k}',n'} | \mathbf{H}_{\mathbf{k},n} \rangle = V_{BZ}\delta_{n,n'}\delta(\mathbf{k}'-\mathbf{k})$, where $V_{BZ}=(2\pi)^3/V$ is the volume of the first Brillouin zone in the reciprocal space and V is the volume of the real-space unit cell. For each band of the PC, one can construct a Wannier function $\mathbf{W}_n(\mathbf{r})$ as a localized superposition of Bloch functions of the band according to

$$\mathbf{W}_n(\mathbf{r}) = \frac{1}{V_{BZ}}\int_{BZ} d\mathbf{k}\, \mathbf{H}_{\mathbf{k},n}(\mathbf{r}). \tag{2}$$

In the superposition, the phase of Bloch functions $\mathbf{H}_{\mathbf{k},n}$ can be chosen such that the Wannier function $\mathbf{W}_n(\mathbf{r})$ is strongly localized around $\mathbf{r}=0$ with an exponential decay far from $\mathbf{r}=0$. The Wannier functions satisfy the orthogonality conditions $\langle \mathbf{W}_{n'}(\mathbf{r}-\mathbf{R}')|\mathbf{W}_n(\mathbf{r}-\mathbf{R})\rangle = \delta_{n,n'}\delta_{\mathbf{R},\mathbf{R}'}$, and the following relationship can be easily proven:

$$\langle \mathbf{W}_{n'}(\mathbf{r}-\mathbf{R}')|\, \nabla \times \left(\frac{1}{\epsilon}\nabla \times\right)|\mathbf{W}_n(\mathbf{r}-\mathbf{R})\rangle = \delta_{n,n'}\theta_{n,\mathbf{R}'-\mathbf{R}}, \tag{3}$$

where $\theta_{n,\mathbf{R}}$ is the Fourier expansion coefficient of the dispersion curve $\omega_n^2(\mathbf{k})$ of the band, $\theta_{n,\mathbf{R}} \equiv (1/V_{BZ})\int_{BZ} d\mathbf{k}\, \omega_n^2(\mathbf{k})\exp(-i\mathbf{k}\cdot\mathbf{R})$, i.e., $\omega_n^2(\mathbf{k}) = \Sigma_{\mathbf{R}}\theta_{n,\mathbf{R}} \exp(i\mathbf{k}\cdot\mathbf{R})$. We then look for a spatiotemporal wave packet, which is a solution to Eq. (1), as a superposition of translated Wannier functions localized at the different lattice points $\mathbf{R}$ of the periodic structure, with amplitudes $f(\mathbf{R},t)$ that depend on the lattice point $\mathbf{R}$ and can vary in time, i.e., we set

$$\mathbf{H}(\mathbf{r},t) = \sum_{\mathbf{R}} f(\mathbf{R},t)\mathbf{W}_n(\mathbf{r}-\mathbf{R}). \tag{4}$$

Note that, as we consider a pure periodic structure without defects and neglect perturbation terms in Eq. (1) (e.g., nonlinearities), coupling among different bands does not occur and in Eq. (4) the sum can be taken over a single band, of index n. Coupled-mode equations for the temporal evolution of the amplitudes $f(\mathbf{R},t)$ of Wannier functions at different lattice points can be obtained after substitution of Eq. (4) into Eq. (1), taking the scalar product with $\mathbf{W}_n(\mathbf{r}-\mathbf{R})$ and using the orthogonality conditions of Wannier functions, together with Eq. (3). One obtains

$$\frac{\partial^2 f(\mathbf{R},t)}{\partial t^2} + \sum_{\mathbf{R}'} \theta_{n,\mathbf{R}'-\mathbf{R}}\, f(\mathbf{R}',t) = 0. \tag{5}$$

The solution to the coupled-mode equations (5) can be expressed as $f(\mathbf{R},t)=f(\mathbf{r}=\mathbf{R},t)$, where the *continuous* function $f(\mathbf{r},t)$ of space $\mathbf{r}$ and time t satisfies the partial differential equation:

$$\frac{\partial^2 f(\mathbf{r},t)}{\partial t^2} + \omega_n^2(-i\nabla_{\mathbf{r}})f(\mathbf{r},t) = 0, \tag{6}$$

and $\omega_n^2(-i\nabla_{\mathbf{r}})$ is the operator obtained after the substitution $\mathbf{k}\rightarrow -i\nabla_{\mathbf{r}}$ in the Fourier expansion of $\omega_n^2(\mathbf{k})$. It should be noted that the differential equation for the *continuous envelope* $f(\mathbf{r},t)$ of the Wannier function wavepacket [Eq. (4)], as given by Eq. (6), is exact, and for any band of the PC an envelope equation can be written, the specific details of the band entering both in the dispersion curve $\omega_n^2(\mathbf{k})$ and in the shape of the corresponding Wannier function $\mathbf{W}_n$ [Eq. (2)].

III. SPATIAL AND SPATIOTEMPORAL LOCALIZED WAVES

The most general solution to the Wannier-function envelope equation (6) is given by a superposition of functions $\psi(\mathbf{r},\pm t)$, where $\psi(\mathbf{r},t)$ is a solution to the wave equation:

$$i\frac{\partial \psi}{\partial t} = \omega_n(-i\nabla_{\mathbf{r}})\psi. \tag{7}$$

We are now interested on the search for localized solutions to Eq. (7) such that $|\psi|$ corresponds to a wave propagating undistorted with a group velocity v_g. To this aim, let us set $\psi(\mathbf{r},t)=g(\mathbf{r},t)\exp(i\mathbf{k}_0\cdot\mathbf{r}-i\Omega t)$, where $\mathbf{k}_0$ is chosen inside the first Brillouin zone in the reciprocal space and the frequency Ω is chosen close to (but not necessarily coincident with) $\omega_0=\omega_n(\mathbf{k}_0)$. The envelope g then satisfies the wave equation

$$i\frac{\partial g}{\partial t} = [\omega_n(\mathbf{k}_0 - i\nabla_{\mathbf{r}}) - \Omega]g. \tag{8}$$

We first note that, if g varies slowly with respect to the spatial variables $\mathbf{r}$, at leading order one can expand $\omega_n(\mathbf{k}_0 - i\nabla_{\mathbf{r}})$ up to first order around $\mathbf{k}_0$; taking $\Omega=\omega_0$, one obtains $\partial g/\partial t + \nabla_{\mathbf{k}}\omega_n\cdot\nabla_{\mathbf{r}} g = 0$, i.e., one retrieves the well-known result for which *an arbitrary* 3D spatially-localized wave packet travels undistorted, at leading order, with a group velocity given by $\nabla_{\mathbf{k}}\omega_n$. Nevertheless, higher-order terms are generally responsible for wave packet spreading, both in space and time. In order to find propagation-invariant envelope waves *even when dispersive terms* are accounted for, let us assume, without loss of generality, that $(\partial\omega_n/\partial k_y)_{\mathbf{k}_0} = (\partial\omega_n/\partial k_z)_{\mathbf{k}_0} = 0$, i.e., let us choose the orientation of the x axis such that the wave packet group velocity $\nabla_{\mathbf{k}}\omega_n$ is directed along this axis, and let us look for a propagation-invariant solution to Eq. (8) of the form $g=g(x_1,x_2,x_3)$, with $x_1=x-v_g t$, $x_2=y$, and $x_3=z$, traveling along the x axis with a group velocity v_g, which is left undetermined at this stage. The function g then satisfies the following equation:

$$-iv_g\frac{\partial g}{\partial x_1} = [\omega_n(\mathbf{k}_0 - i\nabla_{\mathbf{x}}) - \Omega]g, \tag{9}$$

whose solution can be written formally as

$$g(x_1,x_2,x_3) = \int dQ_2\, dQ_3\, G(Q_2,Q_3)\exp(i\mathbf{Q}\cdot\mathbf{x}). \tag{10}$$

In Eq. (10), $\mathbf{x}=(x_1=x-v_g t, x_2=y, x_3=z)$, $\mathbf{Q}=(Q_1,Q_2,Q_3)$, G is an arbitrary spectral amplitude, and $Q_1=Q_1(Q_2,Q_3)$ is implicitly defined by the following *dispersion relation:*

$$\omega_n(\mathbf{k}_0+\mathbf{Q}) - \Omega - v_g Q_1 = 0. \tag{11}$$

To avoid the occurrence of evanescent (exponentially-growing) waves, the integral in Eq. (10) is extended over the values of (Q_2,Q_3) such that Q_1, obtained after solving Eq. (11), turns out to be real-valued. We note that, for an *arbitrary* spectral amplitude G, Eq. (10) represents an *exact* solution of the Wannier-function envelope equation, which propagates *undistorted* with a group velocity v_g, once the proper band dispersion curve $\omega_n(\mathbf{k})$ of the PC and corre-

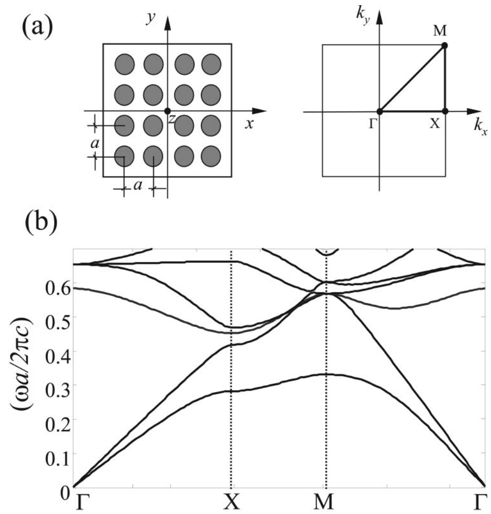

FIG. 1. (Color online) (a) Structure of a square lattice PC (made of cylinders embedded in air) and first Brillouin zone in the reciprocal plane, with the triangular irreducible zone with high-symmetry points Γ, X, and M. (b) Dispersion curves of TE and TM modes for $r=0.2a$ and $\epsilon=8.9$. The blue curve in the figure (the third one from the bottom) corresponds to the second band for TM modes (TM airband).

sponding dispersion relation (11) are computed, e.g., by numerical methods. For *some* specific choices of the spectral amplitude G, in addition to undistorted wave propagation a certain degree of spatiotemporal wave localization can be obtained. It is worthwhile to get some explicit examples, though approximate, of such 3D localized waves, admitting the integral representation given by Eq. (10), and relate them to already known localized solutions to canonical wave equations [2]. To this aim, we develop an asymptotic analysis of Eq. (11) by assuming that the spectral amplitude G is nonvanishing in a narrow interval around $Q_2=Q_3=0$, so that, for Ω close to ω_0, the value of Q_1, as obtained from Eq. (11), is also close to $Q_1=0$. In this case, an approximate expression for the dispersion relation $Q_1=Q_1(Q_2,Q_3)$ can be obtained by expanding in Eq. (11) the band dispersion curve $\omega_n(\mathbf{k}_0+\mathbf{Q})$ at around $\mathbf{k}_0$. We should distinguish two cases, depending on the value of the group velocity v_g, which is basically a free parameter in our analysis.

First case. The first case corresponds to the choice of a group velocity v_g different from (and enough far from) $\partial\omega_n/\partial k_x$. In this case, the leading-order terms entering in Eq. (11) after a power expansion of $\omega_n(\mathbf{k}_0+\mathbf{Q})$ are quadratic in Q_2, Q_3 and linear in Q_1; precisely, one has

$$\left(\frac{\partial\omega_n}{\partial k_1}-v_g\right)Q_1+\omega_0-\Omega+\frac{1}{2}\sum_{i,j=2}^{3}\frac{\partial^2\omega_n}{\partial k_i\,\partial k_j}Q_iQ_j=0, \quad (12)$$

where $k_i=k_{x,y,z}$ for $i=1,2,3$ and the derivatives of the band dispersion curve are calculated at $\mathbf{k}=\mathbf{k}_0$. If the approximate expression of Q_1, given Eq. (12), is introduced into Eq. (10), one can easily show that the envelope $g(x_1,x_2,x_3)$ satisfies the differential equation:

$$i\left(\frac{\partial\omega_n}{\partial k_1}-v_g\right)\frac{\partial g}{\partial x_1}=(\omega_0-\Omega)g-\frac{1}{2}\sum_{i,j=2}^{3}\frac{\partial^2\omega_n}{\partial k_i\,\partial k_j}\frac{\partial^2 g}{\partial x_i\,\partial x_j}. \quad (13)$$

Since the matrix $\partial^2\omega_n/\partial k_i\,\partial k_j$ is symmetric, after a suitable rotation of the (x_2,x_3) axes by the transformation $x'_j=\mathcal{R}_{ji}x_i$ $(i,j=2,3)$, where $\mathcal{R}_{ji}$ is the orthogonal matrix that diagonalizes $\partial^2\omega_n/\partial k_i\,\partial k_j$, assuming without loss of generality $\Omega=\omega_0$, Eq. (13) can be written in the canonical Schrödinger-like form:

$$i\left(\frac{\partial\omega_n}{\partial k_1}-v_g\right)\frac{\partial g}{\partial x_1}=-\frac{1}{2}\alpha_2\frac{\partial^2 g}{\partial x_2'^2}-\frac{1}{2}\alpha_3\frac{\partial^2 g}{\partial x_3'^3}, \quad (14)$$

where α_2 and α_3 are the eigenvalues of the 2×2 matrix $\partial^2\omega_n/\partial k_i\,\partial k_j$ $(i,j=2,3)$. 3D localized waves to Eq. (14) are expressed in terms of well-known Gauss-Hermite functions, which are in general anisotropic for $\alpha_2\neq\alpha_3$. These 3D localized waves, which exist regardless of the sign of α_2 and α_3, represent Gaussian-like beams, with exponential localization in the transverse (y,z) plane and algebraic localization, determined by the beam Rayleigh range, in the longitudinal x direction (and hence in time). These beams propagate undistorted along the x direction with an *arbitrary* group velocity v_g, either subluminal or superluminal, provided that $v_g\neq\partial\omega_n/\partial k_x$. Such pulsed propagating Gaussian beams represent an extension, in a PC structure, of similar solutions found in vacuum (see [18] and references therein). In particular, the special case $v_g=0$ leads to stationary (monochromatic) Gaussian-like beams; note that the condition $v_g\neq\partial\omega_n/\partial k_x$ implies that such steady Gaussian beams do not exist in a PC close to a bandgap edge, where $\partial\omega_n/\partial k_x$ vanishes. Other solutions to Eq. (14), leading to *spatial* 2D localized and monochromatic waves in the transverse (y,z) plane (but delocalized in the longitudinal x direction), can be search in the form $g(x_1,x_2,x_3)=s(x_2,x_3)\exp(i\lambda x_1)$, where λ is a propagation constant. If α_2 and α_3 have the same sign, the function $s(x_2,x_3)$ satisfies a 2D Helmholtz equation, admitting well-known Bessel-beam solutions in cylindrical coordinates. For $\alpha_2\neq\alpha_3$, such solutions are anisotropic, and again they represent a generalization to a PC of well-known spatial Bessel beams in vacuum. If α_2 and α_3 have opposite sign, one obtains a hyperbolic 2D equation (or, equivalently, a 1D Klein-Gordon equation), which admits to 2D X-type localized solutions involving modified Bessel functions recently studied in [9] [see Eqs. (3a) and (4) of Ref. [9]; see also Ref. [19]].

Second case. The second case corresponds to the choice $v_g=\partial\omega_n/\partial k_x$. In this case, the leading-order approximation to the dispersion relation [Eq. (11)] should include also second-order derivatives with respect to x_1 of the band dispersion curve $\omega_n(\mathbf{k}_0+\mathbf{Q})$, yielding

$$\omega_0-\Omega+\frac{1}{2}\sum_{i,j=1}^{3}\frac{\partial^2\omega_n}{\partial k_i\,\partial k_j}Q_iQ_j=0, \quad (15)$$

where the derivatives of the band dispersion curve are calculated at $\mathbf{k}=\mathbf{k}_0$. If the approximate expression of Q_1, implicitly defined by the quadratic equation (15), is introduced into

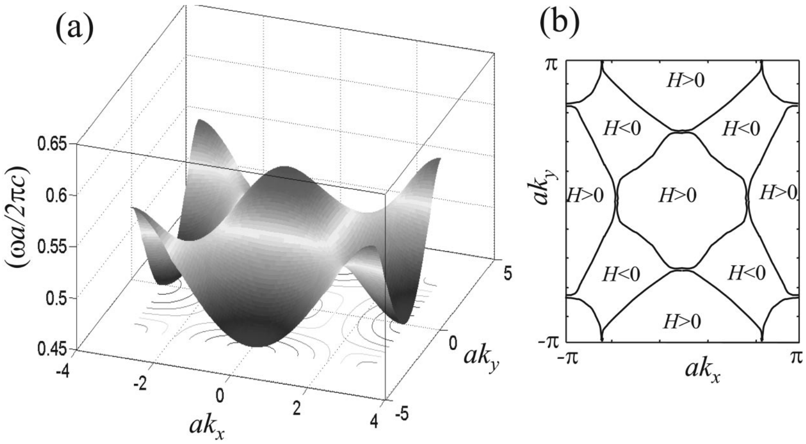

FIG. 2. (Color online) (a) Surface diagram of PC band $\omega_n(k_x, k_y)$ for the TM airband of Fig. 1(a). (b) Sign of the Hessian $H = \det(\partial^2\omega_n/\partial k_i\,\partial k_j)$ for the TM airband (the continuous lines correspond to $H=0$).

Eq. (10), one can easily show that the envelope $g(x_1, x_2, x_3)$ satisfies this time the differential equation:

$$(\omega_0 - \Omega)g = \frac{1}{2}\sum_{i,j=1}^{3} \frac{\partial^2\omega_n}{\partial k_i\,\partial k_j}\frac{\partial^2 g}{\partial x_i\,\partial x_j}. \tag{16}$$

Since the matrix $\partial^2\omega_n/\partial k_i\,\partial k_j$ is symmetric, after a suitable rotation of the (x_1, x_2, x_3) axes by the transformation $x_j' = \mathcal{R}_{ji}x_i$ $(i,j=1,2,3)$, where $\mathcal{R}_{ji}$ is the orthogonal matrix that diagonalizes $\partial^2\omega_n/\partial k_i\,\partial k_j$, Eq. (16) takes the canonical form:

$$(\omega_0 - \Omega)g = \frac{1}{2}\left(\alpha_1\frac{\partial^2 g}{\partial x_1'^2} + \alpha_2\frac{\partial^2 g}{\partial x_2'^2} + \alpha_3\frac{\partial^2 g}{\partial x_3'^3}\right), \tag{17}$$

where α_i $(i=1,2,3)$ are the eigenvalues of the 3×3 matrix $\partial^2\omega_n/\partial k_i\,\partial k_j$ $(i,j=1,2,3)$. The sign of the eigenvalues α_i basically determines the elliptic or hyperbolic character of Eq. (17), and hence the nature of their solutions (see, e.g., [2]). If α_i have the same sign, e.g., they are positive, for $\Omega < \omega_0$ Eq. (17) reduces, after a scaling of axis length, to a 3D Helmholtz equation, which in spherical coordinates admits of localized solutions in the form of sinc-shaped waves (see, e.g., [2,5]). If, conversely, there is a sign discordance among the eigenvalues α_i, one obtains a 2D Klein-Gordon equation, which admits of 3D localized X-type waves which have been lengthly discussed in many works (see, e.g., [2,6,9] and references therein). In some special cases, one of the eigenvalues α_i may vanish, which may yield further nonspreading wave packet solutions. Notably, if $\alpha_1=0$, the solution to Eq. (17) is given by $g(x_1,x_2,x_3)=h(x_1)\varphi(x_2,x_3)$, where h is an arbitrary function of $x_1 = x - v_g t$ and φ satisfies a 2D Helmholtz equation for $\alpha_2\alpha_3 > 0$, admitting Bessel beam solutions, or a 1D Klein-Gordon equation for $\alpha_2\alpha_3 < 0$, admitting 2D X-type solutions. For these special solutions a cancellation of temporal dispersion is attained. As the former case $(\alpha_2\alpha_3 > 0)$ extends to a PC structure the so-called pulsed Bessel beams found in homogeneous dispersive media [3], the latter case $(\alpha_2\alpha_3 < 0)$ is rather peculiar for a PC structure,

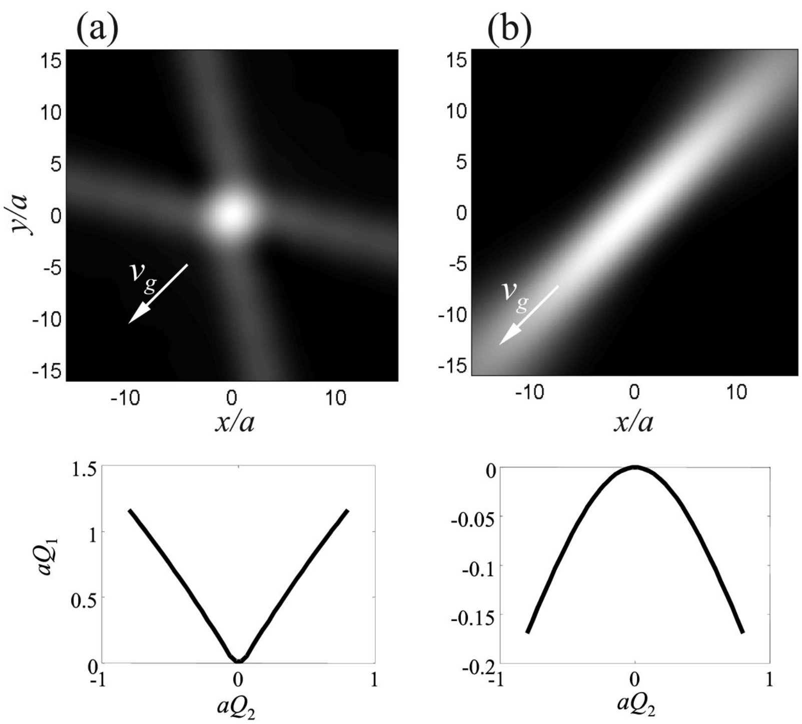

FIG. 3. Gray-scale plots of localized propagating waves as obtained from Eq. (18) for a Gaussian spectral amplitude with $\lambda = 2a$ and for $\mathbf{k}_0 = (1.6/a)(\mathbf{u}_{\mathbf{k}x} + \mathbf{u}_{\mathbf{k}y})$ and $\Omega = \omega_n(\mathbf{k}_0) \simeq 0.5338(2\pi c/a)$ (see text). In (a) $v_g = |\boldsymbol{\nabla}_{\mathbf{k}}\omega_n| \simeq 0.0532c$ (hyperbolic localization), whereas in (b) $v_g = c$ (parabolic localization). The bottom figures show, for the two cases, the corresponding dispersion relation $Q_1 = Q_1(Q_2)$ as numerically computed by solving Eq. (11).

which realizes a bidiffractive propagation regime [9], i.e., positive and negative diffraction along the two transverse directions y and z. Instead of pulses with a transverse Bessel beam profile, in this case one obtains a transverse X-shaped beam with an arbitrary longitudinal (temporal) profile that propagates without spreading.

We note that, though our analysis has been focused to a 3D PC, similar results can be obtained *mutatis mutandis* for the lower-dimensional case of a 2D PC. In this case, not considering out-of-plane propagation, the fields depend solely on the two spatial variables x and y defining the PC plane, and the most general solution to the Wannier function envelope equation (8) propagating undistorted with a group velocity v_g along the x axis reads

$$g(x_1,x_2) = \int dQ_2\, G(Q_2)\exp(iQ_1x_1 + iQ_2x_2), \qquad (18)$$

where $x_1=x-v_gt$, $x_2=y$, G is an arbitrary spectral amplitude, and $Q_1=Q_1(Q_2)$ is implicitly defined again by the dispersion relation given by Eq. (11). Depending on the value of the group velocity v_g as compared to $\partial\omega_n/\partial k_x$, the scenario discussed for the 3D case still holds. In particular, for v_g different from (and enough far from) $\partial\omega_n/\partial k_x$, the lowest order differential equation describing undistorted wave propagation is a 1D Schrödinger equation—given by Eq. (14) where the last term on the right-hand side is dropped—which admits of 1D Gauss-Hermite solutions (*parabolic* localization regime). Conversely, for $v_g=\partial\omega_n/\partial k_x$, the lowest-order differential equation describing undistorted spatiotemporal wave propagation is given by Eq. (17) provided that the terms containing the derivatives $\partial/\partial x_3'$ are dropped. In this case, Eq. (17) corresponds to either a 2D Helmholtz equation or to a 1D Klein-Gordon equation, depending whether the Hessian $H=\det(\partial^2\omega_n/\partial k_i\partial k_j)$ is positive or negative. In the former case (*elliptic* localization regime), typical localized solutions in cylindrical coordinates are expressed by Bessel functions of first kind, whereas in the latter case (*hyperbolic* localization regime) X-type wave localization is achieved (see, e.g. [9,19]).

As an example of undistorted spatiotemporal wave propagation, let us consider a simple 2D PC structure made of a square lattice of cylinders, with radius r and period a, embedded in air [see Fig. 1(a)]. A few low-order dispersion bands for TE and TM modes of the PC, as obtained by a standard plane-wave expansion technique, are shown in Fig. 1(b) for parameter values corresponding to alumina ($\epsilon=8.9$) and $r=0.2a$ (see also Fig. 2 in Chap. 5 of Ref. [20]). The computation and shape of Wannier functions for a 2D square lattice PC have been reported in Ref. [15]; here we focus on the construction of undistorted spatiotemporal localized waves of the Wannier function envelope by a direct numerical computation of the integral entering in Eq. (18), which requires solely the numerical computation of the band dispersion curve $\omega_n(k_x,k_y)$ and—through Eq. (11)—of the dispersion relation $Q_1=Q_1(Q_2)$. As an example, let us consider the second TM band in Fig. 1(b), the so-called TM air-band; the entire 2D band surface $\omega_n(k_x,k_y)$ of this band is shown in Fig. 2(a). Figure 2(b) shows the regions in the reciprocal $\mathbf{k}$ space within the first Brillouin zone corresponding to $H>0$ (elliptic localization) or $H<0$ (hyperbolic localization). For a fixed $\mathbf{k}_0$ point, parabolic localization, supporting stationary or propagating 1D Gaussian-like beams, is attained whenever $\mathbf{v}_g$ is far from $\nabla_{\mathbf{k}}\omega_n$; for $\mathbf{v}_g=\nabla_{\mathbf{k}}\omega_n$, localization is instead of hyperbolic or elliptic kind depending on whether $H<0$ or $H>0$. As an example, Fig. 3 shows examples of undistorted waves as obtained from Eq. (11) at point $\mathbf{k}_0=(1.6/a)(\mathbf{u}_{\mathbf{k}x}+\mathbf{u}_{\mathbf{k}y})$—on the ΓM diagonal, where the group velocity is directed along the bisection line of the (x,y) plane—for two different values of the group velocity and assuming a Gaussian spectral amplitude profile $G(Q_2)=\exp[-(\lambda Q_2)^2]$. In the same figure, the dispersion relations $Q_1=Q_1(Q_2)$, as obtained by numerical solution of Eq. (11), are also depicted. Note that at $\mathbf{k}=\mathbf{k}_0$, one has $\nabla_{\mathbf{k}}\omega_n\simeq -0.0532c\mathbf{n}$ and $H<0$, where $\mathbf{n}=(1/\sqrt{2})(\mathbf{u}_x+\mathbf{u}_y)$ is the unit vector of the bisection line of (x,y) plane. Figure 3(a) corresponds to $\mathbf{v}_g=\nabla_{\mathbf{k}}\omega_n$, leading—as expected for a hyperbolic localization regime—to an X-shaped wave. Conversely, in Fig. 3(b) we have chosen the group velocity $\mathbf{v}_g=-c\mathbf{n}$, leading to a Gaussian-like beam propagating at a luminal velocity.

IV. CONCLUSIONS

In conclusion, a general analysis of wave packet propagation in PCs, based on a Wannier function expansion approach, has been presented, and an exact envelope equation describing undistorted propagation of spatiotemporal localized waves has been derived. An asymptotic analysis of the envelope equation shows that a wide class of localized (either spatial or spatiotemporal) waves exist, including propagating Gaussian beams, 2D and 3D X-type waves, sinc-shaped waves, pulsed Bessel beams, and pulsed 2D X waves, some of which have been recently studied with reference to some specific models [8,9].

[1] J. Durnin, J. J. Miceli, and J. H. Eberly, Phys. Rev. Lett. **58**, 1499 (1987); J. Lu and J. F. Greenleaf, IEEE Trans. Ultrason. Ferroelectr. Freq. Control **39**, 441 (1992); P. Saari and K. Reivelt, Phys. Rev. Lett. **79**, 4135 (1997); H. Sõnajalg, M. Ratsep, and P. Saari, Opt. Lett. **22**, 310 (1997); E. Recami, Physica A **252**, 586 (1998).

[2] R. Donnelly and R. W. Ziolkowski, Proc. R. Soc. London, Ser. A **440**, 541 (1993); I. M. Besieris, M. Abdel-Rahman, A. Shaarawi, and A. Chatzipetros, Prog. Electromagn. Res. **19**, 1 (1998).

[3] M. A. Porras, Opt. Lett. **26**, 1364 (2001).

[4] M. A. Porras, S. Trillo, and C. Conti, Opt. Lett. **28**, 1090 (2003); S. Orlov, A. Piskarskas, and S. Stabinis, *ibid.* **27**, 2167 (2003); M. A. Porras, G. Valiulis, and P. Di Trapani, Phys. Rev.

E **68**, 016613 (2003); M. A. Porras and P. Di Trapani, *ibid.* **69**, 066606 (2004).

[5] S. Longhi, Phys. Rev. E **68**, 066612 (2003); Opt. Lett. **29**, 147 (2004).

[6] C. Conti, S. Trillo, P. Di Trapani, G. Valiulis, A. Piskarskas, O. Jedrkiewicz, and J. Trull, Phys. Rev. Lett. **90**, 170406 (2003); C. Conti, Phys. Rev. E **68**, 016606 (2003).

[7] P. Di Trapani, G. Valiulis, A. Piskarskas, O. Jedrkiewicz, J. Trull, C. Conti, and S. Trillo, Phys. Rev. Lett. **91**, 093904 (2003).

[8] C. Conti and S. Trillo, Phys. Rev. Lett. **92**, 120404 (2004).

[9] D. N. Chistodoulides, N. K. Efremidis, P. Di Trapani, and B. A. Malomed, Opt. Lett. **29**, 1446 (2004).

[10] S. Longhi and D. Janner, Phys. Rev. B **70**, 235123 (2004).

[11] H. S. Eisenberg, Y. Silberberg, R. Morandotti, and J. S. Aitchison, Phys. Rev. Lett. **85**, 1863 (2000); T. Pertsch, T. Zentgraf, U. Peschel, A. Bräuer, and F. Lederer, *ibid.* **88**, 093901 (2002).

[12] J. Hudock, N. K. Efremidis, and D. N. Chistodoulides, Opt. Lett. **29**, 268 (2004).

[13] J. P. Albert, C. Jouanin, D. Cassagne, and D. Bertho, Phys. Rev. B **61**, 4381 (2000).

[14] D. M. Whittaker and M. P. Croucher, Phys. Rev. B **67**, 085204 (2003).

[15] A Garcia-Martin, D. Hermann, F. Hagmann, K. Busch, and P. Wölfle, Nanotechnology **14**, 177 (2003).

[16] J. M. Ziman, *Principles of the Theory of Solids*, 2nd ed. (Cambridge University Press, Cambridge, England, 1972), pp. 155–160.

[17] P. Feuer, Phys. Rev. **88**, 92 (1952).

[18] S. Longhi, Opt. Express **12**, 935 (2004).

[19] A. Ciattoni and P. Di Porto, Phys. Rev. E **69**, 056611 (2004).

[20] J. D. Joannopoulos, R. D. Meade, and J. N. Winn, *Photonic Crystals: Molding the Flow of Light* (Princeton University Press, Princeton, NJ, 1995).